Photoemission from the $3d$ and $3p$ subshells of Kr

D. W. Lindle, P. A. Heimann, T. A. Ferrett, P. H. Kobrin,* C. M. Truesdale,†
U. Becker,‡ H. G. Kerkhoff,‡ and D. A. Shirley
Materials and Molecular Research Division, Lawrence Berkeley Laboratory, Berkeley, California 94720
and Department of Chemistry, University of California, Berkeley, California 94720
(Received 15 February 1984; revised manuscript received 26 July 1985)

Partial photoionization cross sections and angular-distribution asymmetry parameters were determined for Kr $3d$ photoemission using photon energies of 100 to 280 eV (to 800 eV for the asymmetry parameter). For the $3p$ subshell, the branching ratio relative to the $3d$ cross section and the asymmetry parameter were measured using energies of 280 to 800 eV. These results show good agreement with Hartree-Fock-theory predictions at all photon energies. The summed intensity of $4p \rightarrow np$ satellites relative to the $3d$ main line was found to be approximately constant in the photon-energy range 180—280 eV, and the average asymmetry parameter for these shake-up states showed a marked increase over the same energy range.

I. INTRODUCTION

Recent photoemission measurements of the $4d$ subshells of Xe (Refs. 1 and 2) and I (in CH_3I) (Ref. 3) have exhibited pronounced oscillations in the energy dependences of partial cross sections and angular distributions caused by interaction of the photoelectron with a centrifugal barrier in the atomic potential. These effects are characterized by a large increase (decrease) in the $4d$ cross section (asymmetry parameter) in the first 30 eV above threshold. They have been attributed[4] to resonant enhancement of the $4d \rightarrow \varepsilon f$ photoionization channel at an energy for which the $l=3$ continuum wave function can penetrate into the inner-well region of the atomic potential, producing good overlap with the bound $4d$ wave function. Related nonresonant effects for high-l continuum channels also may be observed even when no potential barrier exists. For example, $4f$ photoionization in atomic Hg exhibits a "delayed onset" in the $4f \rightarrow \varepsilon g$ cross section,[5] which rises slowly with photon energy for more than 100 eV above threshold. Variations in the asymmetry parameter also are induced in this energy range, although the cross-section and asymmetry-parameter oscillations are not as large as the resonant changes in Xe and I. These nonresonant effects (e.g., in Hg) can be explained[4] by examining the shape of the ionic potential to determine how the strong centrifugal repulsion near the nucleus modifies the dipole amplitude of the high-l continuum channel; as the photoelectron energy increases, the continuum wave function (εg) gradually overcomes the centrifugal repulsion, inducing better overlap with the bound wave function ($4f$).

We report here measurements for the Kr $3d$ subshell that indicate the presence of effects similar to those observed in the Hg $4f$ subshell. Because no centrifugal barrier is present in atomic Kr,[4] the qualitative discussion of delayed onsets outlined above adequately describes the Kr $3d$ cross section, which peaks 90 eV above threshold, and the accompanying changes in the Kr $3d$ asymmetry parameter. In addition to these effects in the dominant $3d$ channel, results for the $3p$ photoemission line and satellites of the $3d$ main line also will be presented.

The experimental method is described in Sec. II, and the results are discussed in Secs. III A and III B for the $3d$ and $3p$ subshells, respectively.

II. EXPERIMENTAL

All of the measurements were made with photons from Beam Line III-1 at the Stanford Synchrotron Radiation Laboratory, using the double-angle time-of-flight (DATOF) method.[2,6,7] The ultrahigh-vacuum monochromator was protected by a 1500-Å-thick Al or 1000-Å-thick C window from the $\sim 10^{-5}$ Torr pressure in the experimental chamber. The monochromator resolution was a fixed 1.3 Å at all energies. The photon beam intersected an effusive gas jet in the interaction region viewed by the apertures of two time-of-flight (TOF) detectors, allowing measurement of photoelectron intensities at two angles and nearly all kinetic energies simultaneously.

For photoionization of a randomly oriented sample by linearly polarized radiation, Yang's theorem[8] defines the differential cross section, $d\sigma/d\Omega$, in the dipole approximation as

$$\frac{d\sigma(h\nu,\theta)}{d\Omega} = \frac{\sigma(h\nu)}{4\pi}[1+\beta(h\nu)P_2(\cos\theta)] \ . \quad (1)$$

In Eq. (1), θ is the angle between the momentum vector of the ejected electron and the polarization vector of the incident radiation, $P_2(\cos\theta)$ is the second Legendre polynomial, and σ and β are the cross section and the angular-distribution asymmetry parameter, respectively, for the photoionization process under study. In this work we assume that the dipole approximation is valid and that the effect of incomplete linear polarization[2] is taken adequately into account by the calibration procedure described in Ref. 6.

Partial cross sections are determined with the DATOF spectrometer by measuring peak intensities as a function of photon energy at $\theta=54.7°$, for which $P_2(\cos\theta)$ van-

ishes, then normalizing to the gas pressure and photon flux. The Kr pressure was monitored by a capacitance manometer on the high-pressure side of the capillary which introduces the gas to the interaction region. It has been determined empirically that the pressure measured in this way is linearly proportional to the gas density encountered by the photon beam over a wide range of pressures. The photon flux was monitored by measuring, with a photomultiplier tube (RCA 8850), the fluorescence intensity of sodium salicylate applied to a quartz window as described by Samson.[9] Previous measurements[10] have indicated that the quantum yield of sodium salicylate is approximately constant for photon energies from 30–107 eV. Recent measurements[11] have shown that the quantum yield increases by about a factor of 2 from ~80 to 270 eV. This result has been corroborated qualitatively by other workers.[12] As a result, the $3d$ cross section reported here has been corrected for this substantial change in the sensitivity of the photon-flux monitor. Because of this correction, we estimate that the relative values of σ_{3d} [i.e., relative to σ_{3d} in the 170–190 eV range, where the partial cross section has been scaled to absorption (see Sec. III A for details)] may vary systematically by as much as ±20%, with the largest error at high energies where the correction is most uncertain. Above 270 eV the sodium salicylate quantum yield is unknown, and no partial cross sections are reported at higher photon energies.

Simultaneous measurement of the relative intensities of two photoelectron peaks at $\theta=54.7°$ yields branching-ratio data that are independent of variations in photon flux and gas pressure. Measurement at one additional angle ($\theta=0°$) yields values of β that are also independent of these changes. We estimate systematic errors to be ±10% for branching ratios and ±0.10 for asymmetry parameters. At certain photon-energy settings of the monochromator, a component of second-order radiation (energy of $2h\nu$) was large enough to produce peaks in our spectra, primarily second-order peaks of Kr $3d$ and $3p$ photoionization. We were able to extend some of our β and branching-ratio results to higher photon energies using this second-order radiation.

III. RESULTS AND DISCUSSION

A TOF spectrum of Kr taken at a photon energy of 224 eV is shown in Fig. 1. This spectrum is dominated by features associated with $3d$ subshell photoionization; the unresolved $3d$ photoemission lines with binding energies of 93.79 eV ($4d_{5/2}$) and 95.04 eV ($4d_{3/2}$),[13] a satellite peak of the $3d$ line, mostly composed of $4p\rightarrow 5p$ shake-up states (~114 eV binding energy[14]), and all of the Auger features below 60 eV kinetic energy. Evidence of $3p$ ionization [thresholds at 214.4 and 222.2 eV (Ref. 15)] is apparent with the $M_{2,3}M_{4,5}N$ Auger peak. The remaining high-energy peaks result from photoionization of the valence shell and from photoemission induced by higher-order components of the synchrotron radiation.

A. $3d$ subshell

The $3d$-cross-section results, after correction for the changing sodium salicylate response, are shown in Fig. 2. The present measurements have been scaled to the total

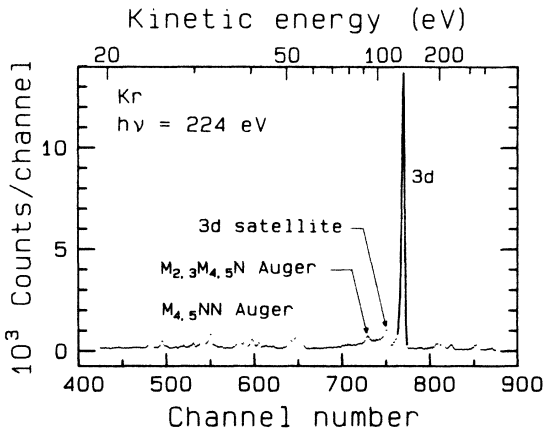

FIG. 1. TOF photoelectron spectrum of Kr at a photon energy of 224 eV and with $\theta=0°$. All of the features below 60 eV are $M_{4,5}NN$ Auger lines. The $3d$ satellite includes all of the $4p\rightarrow np$ shake-up transitions. The peaks to the right of the $3d$ main line arise from valence photoionization and from photoemission induced by second- and higher-order components of the incident radiation.

photoabsorption cross section[16] (σ_{abs}) at 170 and 190 eV photon energy, after consideration of the other available channels contributing to σ_{abs}. The other single-ion final states, valence ($4p$ and $4s$) and correlation satellites of the $3d$ main line, were estimated from the TOF spectra to be 6(1)% and 8(1)% of σ_{3d} in this energy range, respectively. Intensity estimates of photoionization producing double ions (i.e., shake-off) were taken from previous measurements,[17–20] which found that shake-off accompanying valence ionization is 18(1)% of the single-ion valence cross section[17,18,21] (and thereby ~1% of σ_{3d}), and that shake-off accompanying $3d$ ionization is 22(3)% of

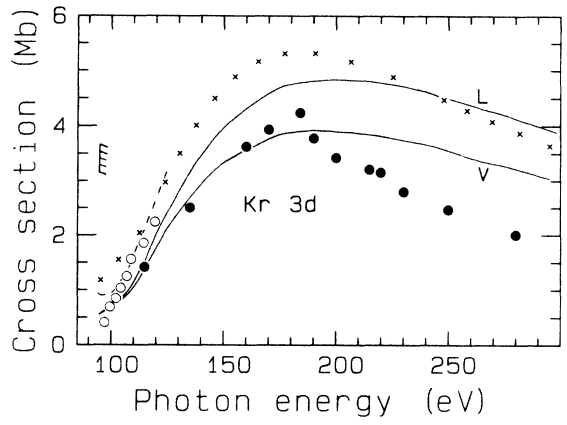

FIG. 2. Partial cross section for Kr $3d$ photoemission. Solid circles are the present results, open circles are from Ref. 22. The ×'s represent the total absorption cross section (Ref. 16). The solid and dashed curves represent HF [length (L) and velocity (V)—Ref. 23] and RRPA (Ref. 24) calculations, respectively, with the RRPA curve shifted 9 eV to lower energy to coincide with the experimental threshold. The present results have been scaled to absorption as described in the text.

σ_{3d}.[18–20] Inclusion of these channels indicates that σ_{3d} is 73(2)% of the total cross section for 170–190 eV photon energy.

Other 3d results are included in Fig. 2. Tentatively, the measurements of Carlson *et al.*[22] near threshold do not agree with our results, although the data overlap is poor. We note also that the more rapid increase in σ_{3d} measured previously[22] may be inconsistent with the slower rise of σ_{abs}, even after consideration of the valence contribution to σ_{abs}. Comparison with theory shows good agreement with a Hartree-Fock velocity (HF-V) calculation[23] up to 200 eV, just below the 3p threshold. Agreement is worse with HF length (HF-L) (Ref. 23) and relativistic random-phase approximation (RRPA) (Ref. 24) calculations, both of which agree somewhat better with the earlier photoemission measurements.[22] However, it is expected[25] that the RRPA calculations will overestimate inner-shell partial cross sections for cases in which appreciable multielectron processes are present (20–25 % for Kr), because the RRPA equations include only single-ionization events while requiring the partial cross sections to sum to the correct total oscillator strength. Consideration of this correction should improve agreement between RRPA theory and experiment for Kr. Finally, HF-L calculations generally are considered better than HF-V,[26] indicating that the better agreement between experiment and the HF-V curve is somewhat fortuitous.

The delayed onset of σ_{3d} is seen clearly in our results. The maximum at 185(10) eV can be ascribed to an interaction of the photoelectron in the εf channel with the repulsive part of the atomic potential.[4] Near threshold, the centrifugal repulsion experienced by an $l=3$ continuum electron inhibits the εf channel. As the energy increases, this channel grows to dominate the photoionization process, inducing a steady increase in the cross section.[27] The position of the σ_{3d} maximum is in good agreement with absorption results.[16]

Figure 3 displays the measured asymmetry parameters for 3d photoionization along with previous measurements by Krause[19] and Carlson *et al.*[22] We observe excellent agreement with the earlier data at all energies. Comparison with HF,[23] RRPA,[24] and Hartree-Slater (HS) (Ref. 28) calculations also is made in Fig. 3. Only one curve is shown because the theoretical results nearly coincide at all energies (the RRPA and HF calculations extend from threshold to 125 and 435 eV, respectively). Agreement among the experimental and theoretical results is very good. The oscillation in β_{3d} has been attributed to the delayed onset in $3d \rightarrow \varepsilon f$ ionization observed in σ_{3d}.[4] The minimum at 135–140 eV photon energy is predicted very well by the HF and HS calculations, thus confirming this interpretation, as well as indicating that Kr 3d photoionization can be described adequately by a one-electron model.

The sum of the intensities of the $\underline{3d}\,\underline{4p}np$ satellites (underlined subshells have a vacancy) relative to the 3d main line is shown in the top of Fig. 4. The $4p \rightarrow np$ satellites were unresolved in the TOF spectra: thus the results in Fig. 4 represent values for all of these peaks combined. Very little is known about the energy-dependent behavior of satellite intensities.[29] Empirically, Wuilleumier and Krause[30] plotted relative satellite intensities against a reduced-energy parameter, ε/E_0, where ε is the kinetic energy of the satellite photoelectron and E_0 is the satellite excitation energy (i.e., the binding energy of the satellite less the binding energy of the main line). For the Kr $\underline{3d}\,\underline{4p}np$ satellites, E_0 is approximately 20 eV, and the reduced-energy region covered by the measurements in Fig. 4 is $3.3 \leq \varepsilon/E_0 \leq 8.3$. In this range one expects the high-energy or sudden limit to be reached,[30] and we observe a fairly constant branching ratio, although there is slight evidence that it may be decreasing at higher energy.

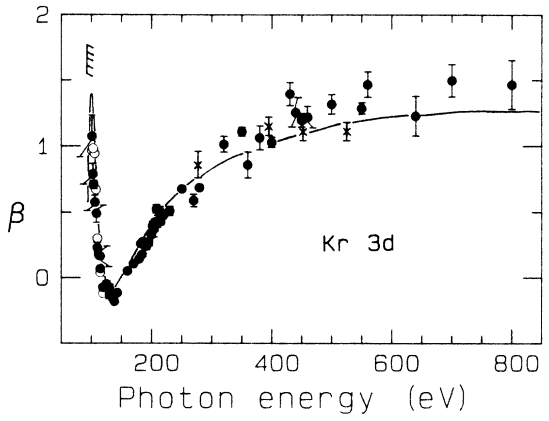

FIG. 3. Angular-distribution asymmetry parameter for Kr 3d photoemission. Solid circles are the present results, open circles and ×'s are from Refs. 22 and 19, respectively. The single curve represents RRPA (Ref. 24), HF (Ref. 23), and HS (Ref. 28) calculations, after the RRPA curve is shifted 9 eV as in Fig. 2. The RRPA calculation extends from threshold to 125 eV and the HF calculation to 435 eV.

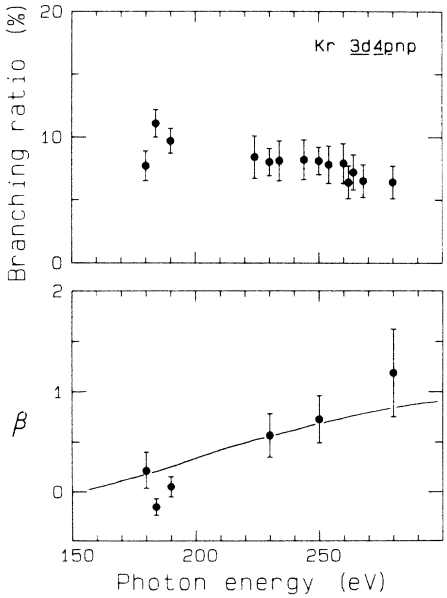

FIG. 4. Intensity relative to the 3d main line (top) and asymmetry parameter (bottom) of the Kr $\underline{3d}\,\underline{4p}np$ satellites. All of the $4p \rightarrow np$ satellites were unresolved and are included in these results. The solid curve in the bottom panel represents β_{3d}.

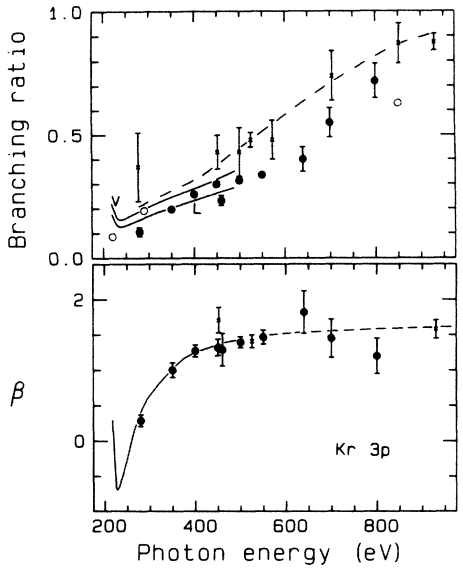

FIG. 5. Branching ratio of Kr $3p$ ionization relative to σ_{3d} (top) and $3p$ asymmetry parameter (bottom). Solid circles are present results, and open circles and $\times$'s are from Refs. 32 and 19, respectively. The results of Ref. 19 in the top panel, which were measured at $\theta=90°$, have been corrected for β_{3p} and β_{3d}. Solid curves are HF calculations (Ref. 23) for the length (L) and velocity (V) formulations. Dashed curves represent HS calculations (Ref. 28). In the bottom panel, the HF length and velocity calculations coincide.

Assuming a constant branching ratio, we find an average value of 8(1)%, which agrees very well with an Al $K\alpha$ measurement[31] of 8(1)% for the sum of the $4p\rightarrow np$ satellites, but disagrees with a higher-resolution Mg $K\alpha$ measurement[14] of 11.7% for these same transitions. The Mg $K\alpha$ value is in better agreement with a theoretical sudden-limit result[14] of 10.6%.

Similarly, little is known about the energy dependence of satellite asymmetry parameters. As a first approximation, one might expect that the satellite β will mimic the asymmetry parameter of the main line. Comparison of the $\underline{3d}\,\underline{4p}np$ asymmetry-parameter results to β_{3d} in the bottom of Fig. 4 shows that both β parameters increase in this energy range, and that the change in the satellite asymmetry parameter is approximately the same as that for β_{3d}.

B. $3p$ subshell

For energies above the Kr $3p$ thresholds (average value of 218 eV), the $3p$ photoionization intensity relative to $3d$ ionization is shown in the top of Fig. 5. As the photon energy increases, σ_{3d} decreases from its maximum due to the delayed onset, making $3p$ ionization relatively more important. Also included in Fig. 5 are previous measurements[19,32] and HF (Ref. 23) and HS (Ref. 28) calculations of the cross-section ratio. Agreement is generally satisfactory.

The $3p$ asymmetry parameter shown in the bottom of Fig. 5 agrees well with previous results.[19] The gradual increase to the asymptotic value of ~ 1.6 (Ref. 19) is predicted well by theory.[23,28] We conclude from these results and from those for σ_{3d} and β_{3d} that inner-shell photoionization in Kr can be described reasonably well within a one-electron model, despite the presence of appreciable multielectron processes in the $3d$ subshell.

ACKNOWLEDGMENTS

This work was supported by the Director, Office of Energy Research, Office of Basic Energy Sciences, Chemical Sciences Division of the U.S. Department of Energy under Contract No. DE-AC03-76SF00098. It was performed at the Stanford Synchrotron Radiation Laboratory, which is supported by the Department of Energy's Office of Basic Energy Sciences. One of us (U.B.) would like to acknowledge support by the Deutsche Forschungsgemeinschaft and another (H.G.K.) would like to acknowledge support by the Wigner foundation.

*Present address: Rockwell Science Center, P.O. Box 1085, Thousand Oaks, CA 91360.

†Present address: Research and Development Division, Corning Glass Works, Corning, NY 14831.

‡Permanent address: Fachbereich Physik, Technische Universität Berlin, 1000 Berlin 12, West Germany.

[1]S. H. Southworth, P. H. Kobrin, C. M. Truesdale, D. Lindle, S. Owaki, and D. A. Shirley, Phys. Rev. A **24**, 2257 (1981).

[2]S. Southworth, U. Becker, C. M. Truesdale, P. H. Kobrin, D. W. Lindle, S. Owaki, and D. A. Shirley, Phys. Rev. A **28**, 261 (1983).

[3]D. W. Lindle, P. H. Kobrin, C. M. Truesdale, T. A. Ferrett, P. A. Heimann, H. G. Kerkhoff, U. Becker, and D. A. Shirley, Phys. Rev. A **30**, 239 (1984).

[4]S. T. Manson and J. W. Cooper, Phys. Rev. **165**, 126 (1968).

[5]P. H. Kobrin, P. A. Heimann, H. G. Kerkhoff, D. W. Lindle, C. M. Truesdale, T. A. Ferrett, U. Becker, and D. A. Shirley, Phys. Rev. A **27**, 3031 (1983).

[6]S. Southworth, C. M. Truesdale, P. H. Kobrin, D. W. Lindle, W. D. Brewer, and D. A. Shirley, J. Chem. Phys. **76**, 143 (1982).

[7]M. G. White, R. A. Rosenberg, G. Gabor, E. D. Poliakoff, G. Thornton, S. Southworth, and D. A. Shirley, Rev. Sci. Instrum. **50**, 1288 (1979).

[8]C. N. Yang, Phys. Rev. **74**, 764 (1948).

[9]J. A. R. Samson, *Techniques of Vacuum Ultraviolet Spectroscopy* (Pied, Lincoln, Nebraska, 1967).

[10]J. A. R. Samson and G. N. Haddad, J. Opt. Soc. Am. **64**, 1346 (1974).

[11]D. W. Lindle, T. A. Ferrett, P. A. Heimann, and D. A. Shirley (unpublished).

[12]J. A. R. Samson (private communication); J. Nordgren and R. Nyholm (private communication).

[13]G. C. King, M. Tronc, F. H. Read, and R. C. Bradford, J. Phys. B **10**, 2479 (1977).

[14]D. J. Bristow, J. S. Tse, and G. M. Bancroft, Phys. Rev. A **25**, 1 (1982).

[15]K. Siegbahn, C. Nordling, G. Johansson, J. Hedman, P. F. Hedén, K. Hamrin, U. Gelius, T. Bergmark, L. O. Werme, R. Manne, and Y. Baer, *ESCA Applied to Free Molecules*

(North-Holland, Amsterdam, 1969).

[16]G. V. Marr and J. B. West, At. Data Nucl. Data Tables **18**, 497 (1976); J. B. West and G. V. Marr, Proc. R. Soc. London, Ser. A **349**, 397 (1976).

[17]J. A. R. Samson and G. N. Haddad, Phys. Rev. Lett. **33**, 875 (1974).

[18]Th.M. El-Sherbini and M. J. Van der Wiel, Physica (Utrecht) **62**, 119 (1972).

[19]M. O. Krause, Phys. Rev. **177**, 151 (1969).

[20]D. M. P. Holland, K. Codling, J. B. West, and G. V. Marr, J. Phys. B **12**, 2465 (1979).

[21]More recent ion-yield measurements have found the double-to-single valence ionization ratio to be 55(9)% (at 80 eV photon energy) (Ref. 20) and ~200% (at 90 eV) (Ref. 33). We propose that these higher ratios, both determined using synchrotron radiation, reflect the presence of second-order radiation at the primary energies of 80 and 90 eV. Note the large 3*d* cross section in Fig. 2 at the secondary energies of 160 and 180 eV, for which the prominent decay channel will produce double ions in an ion-yield experiment.

[22]T. A. Carlson, M. O. Krause, F. A. Grimm, P. R. Keller, and J. W. Taylor, Chem. Phys. Lett. **87**, 552 (1982).

[23]D. J. Kennedy and S. T. Manson, Phys. Rev. A **5**, 227 (1972).

[24]K.-N. Huang, W. R. Johnson, and K. T. Cheng, At. Data Nucl. Data Tables **26**, 33 (1981).

[25]W. R. Johnson (private communication).

[26]S. T. Manson (private communication).

[27]This effect is not a shape resonance, but simply the energy-dependent behavior of 3*d* photoionization into the $l=3$ continuum channel. Related measurements that do involve shape resonances (potential barriers) can be found in Refs. 1—3.

[28]J. W. Cooper and S. T. Manson, Phys. Rev. **177**, 157 (1969).

[29]P. H. Kobrin, S. Southworth, C. M. Truesdale, D. W. Lindle, U. Becker, and D. A. Shirley, Phys. Rev. A **29**, 194 (1984); D. W. Lindle, T. A. Ferrett, U. Becker, P. H. Kobrin, C. M. Truesdale, H. G. Kerkhoff, and D. A. Shirley, *ibid.* **31**, 714 (1985), and references therein.

[30]F. Wuilleumier and M. O. Krause, Phys. Rev. A **10**, 242 (1974).

[31]D. P. Spears, H. J. Fischbeck, and T. A. Carlson, Phys. Rev. A **9**, 1603 (1974).

[32]M. O. Krause and T. A. Carlson, Phys. Rev. **149**, 52 (1966).

[33]T. Hayaishi, Y. Morioka, Y. Kageyama, M. Watanabe, I. H. Suzuki, A. Mikuni, G. Isoyama, S. Asaoka, and M. Nakamura, J. Phys. B **17**, 3511 (1984).